Carbohydrate Polymers 89 (2012) 259–268

Contents lists available at SciVerse ScienceDirect

Carbohydrate Polymers

journal homepage: www.elsevier.com/locate/carbpol

Chemical and biological characterization of pectin-like polysaccharides from the bark of the Malian medicinal tree *Cola cordifolia*

Ingvild Austarheim[a,*], Bjørn E. Christensen[b], Ida K. Hegna[a], Bent O. Petersen[c], Jens O. Duus[c], Ragnar Bye[a], Terje E. Michaelsen[a,d], Drissa Diallo[e], Marit Inngjerdingen[f], Berit S. Paulsen[a]

[a] *School of Pharmacy, University of Oslo, Oslo, Norway*
[b] *NOBIPOL, Department of Biotechnology, NTNU, Trondheim, Norway*
[c] *Carlsberg Laboratories, Copenhagen, Denmark*
[d] *National Institute for Research on Public Health, Oslo, Norway*
[e] *Department of Traditional Medicine, Bamako, Mali*
[f] *IMMI, Faculty of Medicine, University of Oslo, Norway*

ARTICLE INFO

Article history:
Received 15 November 2011
Received in revised form 24 January 2012
Accepted 1 March 2012
Available online 8 March 2012

Keywords:
Cola cordifolia
Pectin
Structure
Rhamnogalacturonan
Immunological activity
Complement system
Cytotoxicity

ABSTRACT

The bark of *Cola cordifolia* used in Malian traditional medicine contains unusual types of polysaccharides with immunomodulating activities. We report for the first time on the structure of a polymer designated CC1P1 having the repeating structure [2→)[α-D-Gal(1→3)]α-L-Rha(1→4)α-D-GalA(1→] as determined by NMR and GC/MS. α-Linked Gal is unusual in pectins. The M_w of 135 kDa was determined by SEC-MALLS. CC1P2 (1400 kDa), another polymer, having the same backbone, but this was substituted with α-4-OMe-GlcA, α-2-OMe-Gal and α-Gal as terminal units. CC1P1 shows a high complement-fixing activity, IC_{50} being 2.2 times lower than the positive pectin control PMII (IC_{50} appr. 71 μg/mL) while IC_{50} of CC1P2 is 1.8 times lower. The simple structure of CC1P1 did not activate macrophages, while CC1P2 (100 μg/mL) showed the same potency as the positive controls PMII (100 μg/mL) and LPS (500 ng/mL). No cytotoxicity was detected.

1. Introduction

The bark of the medicinal tree *Cola cordifolia* (Cav) R. Br. [Sterculiaceae] is widely used in Mali as a remedy for treating wounds, pain, fever, and diarrhea (Diallo et al., 2002; Grønhaug et al., 2008; Togola et al., 2008). For traditional use, the bark of *C. cordifolia* is treated with hot water to prepare a decoction. Numerous kinds of low molecular weight and macromolecular compounds are extracted with hot water and present in the decoction. The presence of the low molecular compounds cannot always explain the activities shown by these herbal drugs. It is therefore possible that at least parts of the activity can originate from the polysaccharides present. This effect might be host mediated via the immune system (Classen, Thude, Blaschek, Wack, & Bodinet, 2006; Kim, Waters, & Burkholder, 2002; Popov, Popova, Ovodova, Bushneva, & Ovodov, 1999; Wagner, Kraus, & Jurcic, 1999; Yamada, Kiyohara, & Marsumoto, 2009), and not a direct effect, often seen by low molecular weight substances. Based on this, we wanted to investigate if the immunomodulating potential of the water-soluble polysaccharides of pectin like nature from *C. cordifolia*, might be responsible for some of the bioactivities of this herbal drug.

Pectins are a group of acidic heteropolysaccharides with a size range of 10–5000 kDa that contains a repertoire of structural complexity associated with at least three specific domains; rhamnogalacturonan I (RG-I), rhamnogalacturonan II (RG-II) and homogalacturonan (HGA) (Perez, Rodriguez-Carvajal, & Doco, 2003). RG-I comprises a backbone of alternating →4)αGalA (1→2) αRha(1→, where a part of the Rha units normally will have a branching point in position 4, but occasionally also in position 3 (Naran, Chen, & Carpita, 2008). The side chains can be of varying size and monosaccharide composition, and can include arabinogalactan type II (AG-II), arabinogalactan type I (AG-I), pure arabinans, pure galactans or other less common side chains. The pectin structure can be important for the activity, as demonstrated in a variety

Abbreviations: Ara, arabinose; Gal, galactose; Rha, rhamnose; GalA, galacturonic acid; 2-OMe-Gal, 2-O-methyl-galactose; 4-OMe-GlcA, 4-O-methyl-glucuronic acid; AG-II, arabinogalactan type II (arabino-3,6-galactans); AG-I, arabinogalactan type I (arabino-4-galactans); RG-I, rhamnogalacturonan type I; PMII, *Plantago major* acidic fraction II; AFM, Atomic force microscopy; AAS, Atomic Absorbance Spectroscopy; SEC-MALLS, Size Exclusion Chromatography – Multi-Angel Laser Light Scattering.

* Corresponding author at: School of Pharmacy, P.O. Box 1068, Blindern, 0316 Oslo, Norway. Tel.: +47 22856569; fax: +47 22854402.
E-mail address: ingvilau@farmasi.uio.no (I. Austarheim).

0144-8617/$ – see front matter © 2012 Elsevier Ltd. All rights reserved.
doi:10.1016/j.carbpol.2012.03.005

of papers written on this subject; for reviews see Yamada and Kiyohara (2007) and Paulsen and Barsett (2005).

A previous study on the pectins present in the bark of *C. cordifolia* by Togola et al. (2008) showed the presence of highly branched polysaccharides with human complement-fixing activity. The polymer mixture showed low solubility and high viscosity, and the fine structure was not fully elucidated. The objective of the present study was to isolate and purify the polymers from the bark of *C. cordifolia*, determine the structure and evaluate the bioactivity by various immunomodulating assays.

2. Experimental

2.1. Material and methods

The bark of *C. cordifolia* (Cav). R Br, (Sterculiaceae) was collected in Kolokani, Mali in 2004. The plant material was identified at the Department of Traditional Medicine and a specimen is deposited as number 1331 in the herbarium at the Department of Traditional Medicines, Bamako, Mali. The plant material was sun-dried and subsequently pulverized in a mechanical grinder to a fine powder (0.1 mm).

2.2. Extraction

The powdered bark of *C. cordifolia* (1440 g) was successively extracted with dichloromethane (DCM) and methanol (MeOH) using a Soxhlet apparatus to remove lipophilic and low molecular weight compounds. The residue (1261 g) was then extracted with 30 L of 50 °C MilliQ water (Millipore Corporation, USA) two times for 1 h followed by centrifugation at 10,000 rpm (15,317 × *g*) in a Heraeus Multifuge 4KR and concentrated to 15 L.

2.3. Purification and initial separation of polysaccharides

The 50 °C extract was applied onto a short DEAE Sepharose fast flow column (5 cm × 2 cm, XK50, GE healthcare, Sweden) to remove colored matter that bound to the surface of the column material. The mobile phase was the water extract itself, and the column was not used for separation, only purification. The extract passing through the column was dialyzed in membrane dialysis tubes, cut off 12–14 kDa, (Spectra/pore, Spectrumlabs, USA) for 72 h against distilled water with frequent changes to remove salts and other low molecular weight substances.

500 mL of the extract (0.5 mg polymer/mL) was then applied on an ANX-Sepharose fast flow 4 (GE-healthcare, Sweden) anion exchange column (XK50, 5 cm × 30 cm, GE healthcare) with Cl^- as counter ion, fitted into an ÄKTA FPLC system (GE-healthcare). The column was first eluted with 2 column volumes (CV) of distilled water followed by a constant NaCl (aq) gradient (0–1 M in 1000 mL). Fractions of 10 mL were collected. The profile of the carbohydrates eluted was monitored by the phenol-sulfuric assay (Dubois, Gilles, Hamilton, Rebers, & Smith, 1956) and the absorbance read (470 nm) on a microtiter plate reader (BIO-RAD, model 3550, USA). The relevant fractions were pooled to obtain sub fractions which were passed through a Chelex 100 solid-phase chelating resin (Sigma–Aldrich) column (2 cm × 20 cm, BioRad, USA) to remove divalent ions. The extracts CC1, CC2 and CC3, were then dialyzed as previously described, see "purification and initial separation of polysaccharides" and lyophilized. Parts of CC1* was used for quantification of amount of divalent ions present before removal. Starch was removed by enzymatic degradation using α-amylase from *Bacillus licheniformis* (Sigma–Aldrich) and β-amylase from sweet potato (Sigma–Aldrich) in combination. The enzymatic treatment was carried out on CC1 in a sodium acetate buffer, pH 4.5 (100 mM), 40 °C for 24 h. A simple iodine test was carried out to see when the reaction was completed.

2.4. Quantification of calcium and magnesium by atomic absorption spectrometry (AAS)(Welz & Sperling, 1999)

Solid samples (200 mg) were decomposed in a mixture of 3.0 mL of conc. nitric acid and 1.0 mL of 30% hydrogen peroxide in a microwave oven. After complete decomposition the solutions were transferred to 50 mL volumetric flasks and filled to volume with distilled water. The contents of calcium and magnesium were determined by atomic absorption spectrometry. A SpectrAA-10BQ (Varian Inc., USA) atomic absorption spectrometer equipped with an acetylene-air burner head was used. The built-in instrument graphics together with an Epson RX-80 printer were used for the recording of the signals and for the construction of the calibration graphs. The instrument parameters were as follows for calcium and magnesium, respectively; wavelength 433.7 and 285.2 nm, slit 0.5 nm for both elements and lamp current 10 and 4 mA. Each solution (standards and samples) was measured 3 times, each time for 5 s. The average of the recorded values was used by the instrument to establish the calibration graph and to calculate the concentrations of calcium and magnesium in the samples.

2.5. Further purification of CC1 on a Mono P column

2.5.1. Analytic chromatography of CC1

1 mL CC1 (2.7 mg/mL) was applied to a prepacked Mono P HR 5/20 (GE-healthcare) column fitted in an ÄKTA FPLC system (GE-healthcare). The column was first eluted isocratic with 4 mL degassed, distilled water and then with a stepwise elution gradient from 0 to 1 M NaCl(aq), step 1; 2 mL with a constant gradient to reach 0.4 M NaCl(aq), step 2; isocratic elution for 4 mL, step 3; constant gradient to reach 1.0 M NaCl (aq) after additionally 8 mL. Fractions of 1 mL were collected. The elution profile was determined by the phenol-sulfuric assay as described above.

2.5.2. Preparative separation of CC1

The analytical procedure was scaled up by using a self packed PBE94 (GE-healthcare) column (XK50, 5 cm × 15 cm), attached into the ÄCTA system. The column was first eluted isocratically with 170 mL distilled, degassed water and then with a stepwise elution gradient from 0 to 1.0 M NaCl (aq), step 1; a vertical gradient step to reach 0.4 M NaCl (aq), step 2; isocratic elution for 170 mL, step 3; a constant gradient to reach 1.0 M NaCl (aq) after 50 mL, step 4; isocratic elution for 150 mL. 5 mL fractions were collected and the elution profile determined using the phenol–sulfuric acid method (Dubois et al., 1956) as described above. The relevant fractions were pooled to obtain sub fractions CC1P1 and CC1P2.

2.6. Visualization of the macromolecules with atomic force microscopy (AFM)

AFM imaging was carried out using a NanoWizard® AFM (JPK Instruments AG, Germany) by intermittent contact mode in air, with Ultrasharp silicon probes (NSC35/AlBS) from MicroMasch (μmasch). Images were obtained with 256 × 256 pixels at a scanning rate of 1 Hz. Prior to visualization, the purified polysaccharides were dissolved in MilliQ water (10 μg/mL) and filtered 0.22 μm (Brand). 10–50 μL of the solution (10–50 ng) was deposited onto the freshly cleaved sheets of the atomically flat mica and the drop was combed slowly once (10–15 s) with a clean cover glass. At the same time, nitrogen was used to dry the already combed part. A filter paper was placed at the end of the mica to remove excessive solution when the glass cover had crossed the mica. After drying with nitrogen for additionally 5 min; the samples were imaged. The

cover glass had been cleaned with 96% ethanol and rinsed well with MilliQ water and dried. All AFM images are shown in height mode, with image processing carried out with JPK Image processing program (JPK instruments AG, Germany), flattening, contrast enhancement and line removing. Air humidity was monitored and stayed between 40 and 60% during imaging.

In order to give the mica a positive charge to trap the negatively charged polysaccharides on the surface for subsequently washing, freshly cleaved mica was mounted inside a dessicator. Vapor deposition of APTES (3-aminopropyltriethoxy silane, Sigma–Aldrich) was carried out by depositing 30 μL solution on a plate inside the dessicator. The mica plates were incubated for 3 h (Limansky, Shlyakhtenko, Schaus, Henderson, & Lyubchenko, 2002).

2.7. Monosaccharide composition

1 mg of a lyophilized polysaccharide was subjected to methanolysis for 20 h (80 °C) using water free 3 M HCl in MeOH (Sigma–Aldrich) (Chambers & Clamp, 1971). 100 μg mannitol was added as an internal standard. The methyl glycosides formed were converted into their corresponding trimethylsilylethers (TMSi) and analyzed by capillary gas chromatography (30 m × 0.32 mm, J&W Scientific Inc.) on a Carlo Erba 6000 Vega Series 2 gas chromatograph with an ICU 600 programmer. The injector temperature was 250 °C, the detector temperature 310 °C and the column temperature was 140 °C when injected, then increased with 1 °C/min to 170 °C, followed by 6 °C/min to 248 °C and then 30 °C/min to 300 °C. Helium was used as carrier gas with a flow rate adjusted to a retention time of 33 min for the internal standard. Based on standards for all the monomers present, the monosaccharides were identified and quantified.

2.8. Detection of arabinogalactan type II (AG-II)

The presence of AG-II was detected by precipitation with the β-glucosyl Yariv reagent by single radial diffusion according to van Holst (van Holst & Clarke, 1985). This reagent interacts with 1→3,6Gal in AG-II chains. This unit is a part of AGP carbohydrate side chains, but precipitate can occur without the presence of protein as long as the 1→3,6 linked galactose units are present.

2.9. Analysis for the presence of acetyl- and methyl esterification

The IR spectra of the polysaccharides in a KBr tablet was registered (Tomoda, Nakatsuk, & Satoh, 1974) and investigated for the presence of absorption bands at 1735 cm^{-1} and 1250 cm^{-1} corresponding to esters.

2.10. Linkage determination by derivatization and GC/MS (methylation analysis)

To distinguish linkages belonging both to 2-OMe-Gal and Gal, the fractions that contained both these monosaccharides were subjected to both ethylation and methylation (Ciucanu & Kerek, 1984). Prior to methylation/ethylation, the uronic acids in the polysaccharides were reduced with $NaBD_4$ to their corresponding deuterated (in position 6) neutral sugars. After methylation/ethylation, the samples were hydrolyzed, reduced, acetylated (Kim & Carpita, 1992) and subsequently the partially methylated or ethylated alditol acetates were analyzed by GC/MS using a Fisons GC 8065 (Fisons instruments) on a SPB-1 fused silica capillary column (30 m × 0.2 mm i.d.) with film thickness 0.20 μm. The injector temperature was 250 °C, the detector temperature 300 °C and the column temperature was 80 °C when injected, then increased with 20 °C/min to 170 °C, followed by 0.5 °C/min to 200 °C and then 30 °C/min to 300 °C. Helium was the carrier gas with a flow rate of 0.9 mL/min. Electron impact ionization was used and mass spectra were obtained using Hewlett-Packard Mass Selective Detector 5970 with a Hewlett-Packard GC. Data was processed with Fisons Masslab. The quantification is based on the results from the monosaccharide composition, see "monosaccharide composition", and effective carbon-response of each compound as detected by the GC/MS experiment (Sweet, Shapiro, & Albersheim, 1975). Weak hydrolysis with 0.2 M TFA for 1 h at 100 °C was applied to the material before the methylation analysis to find out how Rha is linked to GalA in the backbone.

2.11. Molecular weight distribution with SEC-MALLS

Molecular weight distributions of the pectins were determined by two size exclusion chromatography (SEC) columns coupled in series, TSK G 4000PWXL and 3000PWXL (7.8 mm × 300 mm) for analyzing CC2, CC3, CC1P1 and TSK G 6000PWXL and 5000PWXL (7.8 mm × 300 mm) for analyzing CC1P2. Two standards were included, pullulan P-1390 (Hayashibara Biochemical Laboratories, Japan) and alginate 203 kDa (UP-LVG-603-04, FMC NovaMatrix, Norway) analyzed on the same columns as CC1P2. The SEC columns were also coupled to a SIL-10AF autosampler, a LC-10ADvp pump and a SCL-10Avp system controller (Shimadzu, Japan) (Christensen et al., 2001; Vold, Kristiansen, & Christensen, 2006). Three online detectors were used, a multi-angle laser light scattering (MALLS) Dawin Heleos-II (Wyatt, USA), a refractive index detector (Optilab DSP, Wyatt) and a viscometer (ViscoStar, Wyatt). The column was eluted with aqueous 0.05 M Na_2SO_4/0.01 M EDTA, pH 6 at a flow rate of 0.5 mL/min. Pullulan P8 (8 kD) was used for normalization of all the MALLS detectors. 100–150 μL sample solution (0.4–1.5 mg/mL) was injected. All samples were dissolved in distilled water 24 h prior to analysis, and diluted with concentrated eluent to reach eluent concentration before injection. The weight and number average molecular weights (M_w and M_n) were calculated using the ASTRA V (Wyatt) software on the basis of exponential fits of log M vs. V (elution volume). A refractive index increment (dn/dc) of 0.150 was used in the calculations.

2.12. Sequencing of the pectins by NMR

^1H and ^{13}C NMR spectra were recorded on a Bruker Avance 800 MHz spectrometer with a cryoprobe TCI. Wilmad 535 pp high quality NMR tubes were used. The probe temperature was 60 °C (333 K) in order to reduce the viscosity of the samples. The chemical shift of acetone was used as an internal standard (δ_H 2.220 ppm/δ_C 30.89 ppm). The chemical shifts are expressed in δ (ppm) values relative to acetone. The samples, CC1P1 and CC1P2 were dissolved in D_2O (Sigma–Aldrich), 10 mg/mL, with sodium as counter ion. Water suppression was carried out by using excitation sculpting with gradients for all experiments in need of water suppression. All spectra were recorded with phase sensitive detection. The following experiments were recorded; ^{13}C NMR, time domain (TD) 32,768, number of scans (NS) 28,764, ^1H NMR (zgcppr), TD:32768 NS:32, dqCOSY (phase sensitive double quantum filtered correlation spectroscopy), TD:4096/1024, NS:32, TOCSY (total correlation spectroscopy), mixing time 60 ms, TD: 4096/1024, NS:32, NOESY (nuclear Overhauser effect spectroscopy), mixing time; 50 ms, TD: 4096/1024, NS: 32, ^{13}C–^1H-HSQC (heteronuclear single quantum coherence) with decoupling during acquisition, TD:2048/512, NS:64, ^{13}C–^1H-HSQC-NOESY, with decoupling during acquisition, mixing time;100 ms, TD:2048/384, NS: 64, ^{13}C–^1H-HSQC-TOCSY (with decoupling during acquisition) TD:2048/256, NS: 256, ^{13}C–^1H-HMBC (heteronuclear multiple bond correlation), optimized on long range couplings,TD:2048/384, NS:64). All spectra were zero filled in both dimension. TopSpin 2 (Bruker Corporation, USA) were used under acquisition and data processing, and the

freeware Sparky3 (Goddard & Kneller, 2009) was used for keeping track of assignments.

2.13. Complement fixation assay

The human complement-fixing activity was measured by the assay described by Michaelsen, Gilje, Samuelsen, Hagasen, and Paulsen (2000). The assay (Method A) measure the inhibiting of complement mediated hemolysis of red blood cells from sheep sensitized with rabbit anti-sheep red blood cell antibodies. The activity of all the polysaccharide fractions are measured as IC_{50} (lowest concentration giving 50% inhibition of lysis) of PMII (acidic polysaccharide fraction of *Plantago major* (Michaelsen et al., 2000; Samuelsen et al., 1996)) divided on the IC_{50} value for the sample. Data from all the tests are presents as the mean ± S.D. A two tailed, paired Student's *t*-test was employed to compare all the fractions to the positive control (PMII). *P*-values of <0.05 were considered statistically significant.

2.14. Macrophage activation

Nitric oxide (NO) released by activated macrophages is broken down to nitrite (NO_2^-) in the medium, which can be measured in a colorimetric assay using the Griess reagents. The mouse macrophage cell line Raw 264.7 was cultured in RPMI 1640 medium supplemented with 10% fetal bovine serum, antibiotics, L-glutamine, and 5×10^{-5} M 2-mercaptoethanol, and split every second day. Macrophages at a density of 5×10^5 cells/mL were seeded into 96-well flat-bottomed plates, and stimulated for 24 h in duplicates with increasing concentrations of samples, LPS (from *Pseudomonas aeruginosa* 10, Sigma–Aldrich) or the pectic polysaccharide PMII, from *P. major* L. (Samuelsen et al., 1996) as positive controls, or medium alone. Nitrite was then determined in cell-free supernatants. The supernatant (50 μL) was mixed with an equal volume of Griess reagent A (1% [w/v] sulphanilamide in 5% [v/v] phosphoric acid) and incubated at room temperature in the dark for 10 min. After addition of 50 μL 0.1% (w/v) *N*-(1-naphthyl) ethylenediamine dihydrochloride in water (Griess reagent B) the absorbance was measured at 540 nm. A dilution series of $NaNO_2$ was used as a standard reference curve. The experiment was repeated three times, and the results shown are from a representative experiment with mean ± SD.

2.15. Cytotoxicity assay

Lactate dehydrogenase (LDH) released by damaged cells into the cell culture supernatant was determined using LDH cytotoxicity detection kit (Biological Industries, Beit Haemek, Israel), according to the manufacturer's instructions. All the three fractions were tested in the concentrations 125, 250 and 500 μg/mL.

3. Results and discussion

3.1. Isolation and purification of polysaccharides present in the bark of C. cordifolia

The isolation and purification procedure for obtaining pure polysaccharides was performed as described in Fig. 1. The yields for the different fractions are difficult to determined exactly due to some loss during fractionation, but the approximately yields for CC1, CC1P1, CC1P2, CC2 and CC3 were determined to be 70, 50, 20, 20 and 10%, respectively. A part to the aqueous extract, CC1* did not bind to the ANX-anion exchange column although monosaccharide analysis and IR showed that approximately 40% of the monosaccharides present consisted of non esterified uronic acids. For this reason it was decided to investigate if the polymers

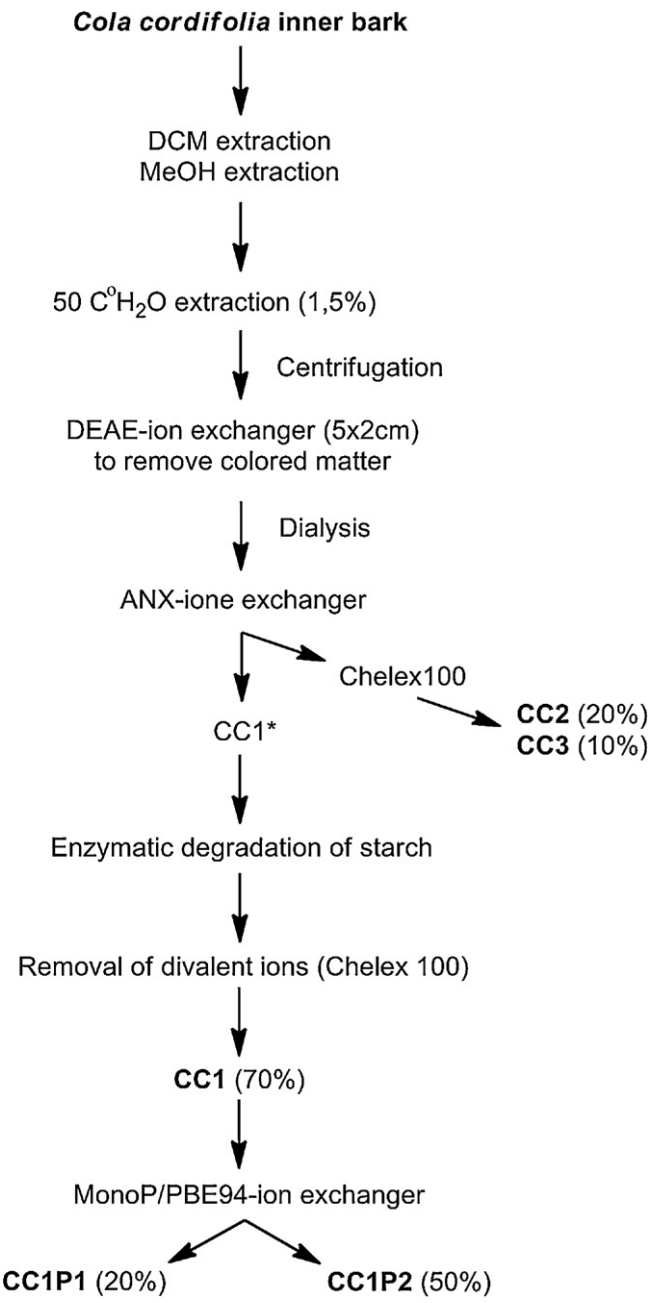

Fig. 1. Purification, separation and isolation scheme for fractionation of CC1, CC1P1, CC1P2, CC2 and CC3. Approximate pectins yields are given in parentheses. CC1, CC2 and CC3 is defined as 100% of the pectins present. Parts of CC1* was used for quantification of divalent ions present in the extract.

could contain high amounts of divalent ions, i.e. Ca^{2+} and/or Mg^{2+} which could explain the lack of binding to an anion exchange column. AAS showed that CC1* contained approximately 0.8% Ca^{2+} and 2.9% Mg^{2+}, a relatively high amount, indicating that these ions may cause ion interactions/crossbinding between the different chains of the polysaccharides giving rise to a higher viscosity and also difficulties of reducing GalA as previously described by Togola et al. (2008). For this reason it was decided to remove the divalent ions before further purification by passing CC1* through a Chelex100 column. This resulted in a decrease in the content of Ca^{2+} and Mg^{2+} to approximately 0.09 and 0.006%, respectively. The dried bark of the tree contained 2.9% Ca^{2+} and 1.8% Mg^{2+}. Prior to the removal of the cations, starch was removed by enzymatic degradation. The amount of Glc in CC1* was decreased from 48 to 1.5%. All polymer

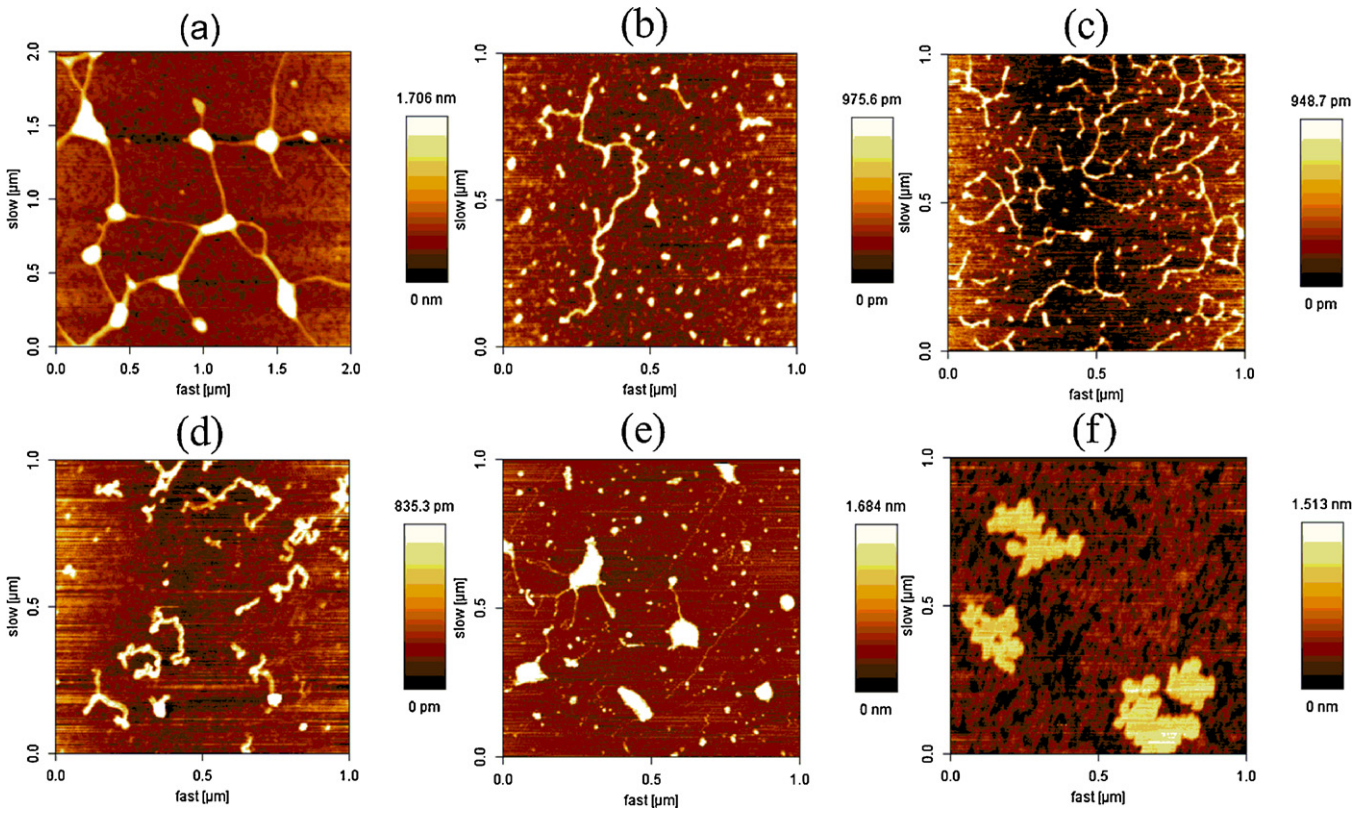

Fig. 2. Topography images of (a) CC1*, (b) CC1, (c) CC1P1, (d) CC1P2, (e) CC3, all scanned on a mica surface, (f) CC1, scanned on an APTES modified mica surface.

fractions contain only minor amounts of protein fractions contain only minor amounts of proteins.

After dialysis, CC1 was applied on a MonoP/PBE94 column. All the polymeric material attached to the column, and CC1P1 and CC1P2 eluted as baseline separated peaks. The fractions CC2 and CC3 attached to the ANX column before removal of divalent ions and were eluted as two peaks, where CC2 eluted before CC3. These two fractions were not possible to separate further on a MonoP column.

3.2. Visualization of the macromolecules

AFM can be used to image individual pectin molecules and to study their aggregation (Morris, Gromer, Kirby, Bongaerts, & Gunning, 2011). The pectins present in the bark of *C. cordifolia* were not methyl-esterified as shown by IR, hence presence of cations like Ca^{2+} and Mg^{2+} are therefore expected to create gelation/aggregation. The uncommon high viscosity observed for CC1* was thought to be a result of the high presence of divalent metal ions shown by AAS. An AFM image of CC1* (Fig. 2a) shows long stretches where no clustering happens, and then regions where there is a clear presence of aggregation. Homogalacturonan (smooth) regions are thought to be important for gelation (egg-box model). The clusters seen might therefore be a result of smooth regions in the pectin. After removal of the divalent ions, the polysaccharides are only present as single threads, and not in condensed areas, see Fig. 2b. The viscosity was significantly reduced as filtration of a 5 mg/mL solution through a 0.22 μm filter (Millipore) now was possible. Before removal of divalent ions, the filtration was only possible through a 5 μm filter (Millipore). Fig. 2c shows polymer chains tangling with each other and also twisting around themselves, but some of the threads were nicely spread out and measured to be more than 400 nm. The height of the threads seems to be between 0.5 and 1 nm, which is in the same area also found by Morris et al. (2011). Fig. 2d, clearly shows the flexible single chains of CC1P2 deposited on the mica as random coils. CC3 diverge from the others as thin single chains are coming out of large condensed clusters, see Fig. 2e. It was impossible to spread the threads out on the mica surface.

The mica surface ($H_2KAl_3(SiO_4)_3$) is negatively charged and will repel the negatively charged pectins. It is therefore impossible to clean the mica after application of the sample which is a normal procedure to remove unwanted particles and salts. We tried therefore to modify the mica surface by using APTES (3-aminopropyltriethoxysilane, Sigma–Aldrich) to make the surface positively charged, thus making the negatively charged polymers attach to the surface. The results are pictured in Fig. 2f. As can be seen from the images, the polymers settled in a different way than for the non-modified mica. Unfortunately, it was impossible to spread the polysaccharides into threads.

3.3. Monosaccharide composition and linkage analysis

The monosaccharide compositions of all fractions are listed in Table 1 and the results from the linkages analysis are listed in Table 2.

The simplest of the polymers are CC1P1 which consists of only three monosaccharides Rha, Gal and GalA, in the approximate ratio 1:1:1. All Gal is terminally linked, all GalA is 1→4 linked and all Rha is 1→2,3 linked. 1→2,3 Rha is an uncommon branching point in plant pectins (Naran et al., 2008). This simple type of polymer has never before been reported, although a similar polymer with 1→2,4 linked Rha and a high degree of acetylation was found in the vegetable okra (Sengkhamparn, Verhoef, Schols, Sajjaanantakul, & Voragen, 2009).

CC1P2 also shows a high degree of branching points in the backbone, indicating relative short side chains. Rha is found both as 1→2,3 linked and 1→2,4 linked monomers in contrast to CC1P1

Table 1
Monosaccharide composition (weight %) and physical parameters of the polysaccharide fractions obtained from the bark of *Cola cordifolia*.

	CC1	CC1P1	CC1P2	CC2	CC3
Ara	3.7[a]	Trace	1.6	37.2	3.0
Rha	22.1	32.0	23.5	8.5	22.8
Gal	20.2	31.0	20.9	31.3	17.3
2-OMe-Gal	6.5	–	6.7	0.4	5.3
4-OMe-GlcA	17.4	–	14.9	6.6	17.8
GalA	29.6	35.0	30.9	11.5	32.8
Glc	0.5	2.0	1.5	1.1	1.0
GlcA				3.4	
AG-II[a]	–	–	–	+	(+)
PDI (M_w/M_n)[b]		1.2	2.6	2.3	3.1
M_w, kDa[c]		135	1400	63	65
M_n, kDa[d]		111	530	28	21

Here, c_i and M_i are the concentrations and molecular weights determined for each elution slice (i) in SEC-MALLS.
[a] The presence of AG-II was determined by β-glucosyl Yariv reagent.
[b] Polydispersity index.
[c] Weight average molecular weight defined as $M_w = \Sigma c_i M_i / \Sigma c_i$.
[d] Number average molecular weight defined as $M_n = \Sigma c_i / (\Sigma c_i / M_i)$.

where only Rha 1→2,3 was detected. The property of CC1P2 is also influenced by the high amount of 4-OMe-GlcA (14.9%) and 2-OMe-Gal (6.7%) present as terminal units, making it more lipophilic because of the methyl groups. The acidic groups will also influence the properties of the pectin, making it more hydrophilic. The presence of 2-OMe-Gal is quite rare in higher plants, as it has only been found in this tree so far. AG-II, which is a common side chain detected in pectins, cannot be detected in CC1P2.

CC2 differs from the rest of the fractions by resembling a more normal pectin structure, containing 15.6% Ara as branching points and 17.8% 1→3,6 linked Gal, commonly found in AG-II. Precipitation with β-glucosyl Yariv reagent (Table 1) confirms this. CC2 has a lower amount of Rha branching in the backbone (2.6%), which indicates longer side chains than those present in CC1P1 and CC1P2.

In CC3, Ara is only present as terminal units; in addition, Gal is mostly present as 1→4 linked Gal (12.2%). This indicates the presence of arabino 4-galactans (AG-I), side chains. Minor amounts of AG-II are also present, showed by a weak positive reaction with the Yariv reagents. This test is very sensitive as CC3 only has 1% 1→3,6 Gal present. Both CC3 and CC1P2, have branching points on GalA which is not detected for CC1P1 or CC2. CC1P2 and CC3 are structurally quite similar, and differ mainly in molecular weights. Branching on GalA might indicate presence of RG-II, but it was not possible to detect the carbohydrate moiety KDO in CC1P2 (results not shown) which means that RG-II is not present.

3.4. Molecular weight distributions

The unimodal RI profile of CC1P1 and relatively low polydispersity (1.2) suggests a relatively uniform type of pectin. The calculated molar mass data (log M vs. V) are almost linear as found for homogeneous polymers. The upturns in molar mass observed at low and high elution volumes were not seen in the corresponding plots of intrinsic viscosity vs. elution volume (not shown), indicating the presence of compact aggregates. Using exponential fits for the molar mass data, weight (M_w) and number average molecular weights (M_n) were calculated, see Table 1. In contrast, the RI peak of CC1P2 is quite broad, indicating some structural heterogeneity (contains subpopulations), but the molar mass data (log M vs. V) are linear except at the tail, where an upturn occurs due to the presence of small amounts of particulate material. CC2 and CC3 show broad RI peaks with multiple shoulders. The calculated molar mass data

Table 2
Linkage determinations of the monomers present in fractions CC1P1, CC1P2, CC2, and CC3. Amounts are given as weight % of the total carbohydrates present.

	Linkage	CC1P1	CC1P2	CC2	CC3
Ara	T_f		1.6	15.9	3.0
	$1\rightarrow3_f$			5.7	
	$1\rightarrow4/5$[a]			9.6	
	$1\rightarrow3,5_f$			3.3	
	$1\rightarrow2,5_f$			2.7	
Rha	T_p			2.7	
	$1\rightarrow2_p$			3.2	5.7
	$1\rightarrow2,3_p$	32.0	15.3	1.1	11.7
	$1\rightarrow2,4_p$		8.2	1.5	5.4
Gal	T_p	31.0	7.9	3.3	4.1
	$1\rightarrow4_p$		13.0	1.8	12.2
	$1\rightarrow3_p$			5.2	
	$1\rightarrow6_p$			3.2	
	$1\rightarrow3,6_p$			17.8	1.0
2-OMe-Gal	T_p		6.7		5.3
4-OMe-GlcA	T_p		14.9	6.6	17.8
GalA	$1\rightarrow4_p$	35.0	23.9	11.5	27.0
	$1\rightarrow3,4_p$		5.7		4.0
	$1\rightarrow2,4_p$		1.3		1.8
GlcA	$1\rightarrow4_p$			3.4	
Glc	$1\rightarrow4_p$	2.0	1.5	1.1	1.0
Terminal units		31.0	31.1	28.5	30.3
Branch points		32.0	30.5	26.4	23.9
Ratio		0.97	1.02	1.08	1.26

[a] It is not possible to distinguish between $1\rightarrow4_p$ and $1\rightarrow5_f$.

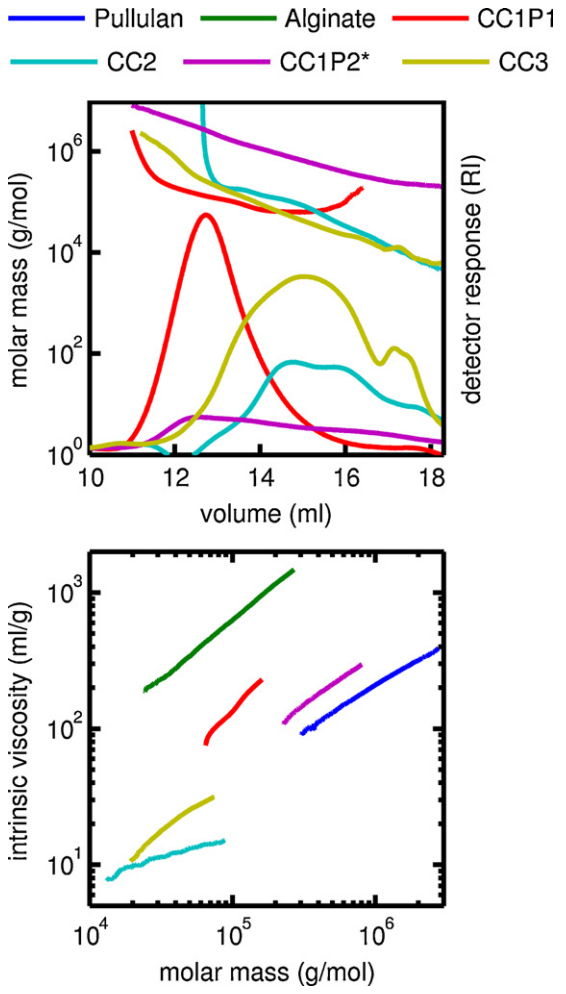

Fig. 3. Results from SEC-MALLS analysis. Left: elution profile (RI detector) and the calculated molar mass of CC2, CC3, CC1P1 and CC1P2. *CC1P2 cannot directly be compared with the rest as different types of columns have been applied. Right: molecular weight dependence of the intrinsic viscosity (MHS-plot). For the sake of comparison, data for alginate and pullulan P1390 are included.

are not strictly linear suggesting that they are heterogeneous, i.e. existing in different geometries in addition to being polydisperse.

Analysis of the relationship between the intrinsic viscosity and the molar mass, also called Mark–Houwink–Sakurada (MHS) plots, see Fig. 3, provides further information about the physical shape and extension of the chains (in solution). Intrinsic viscosities were obtained for each elution slice using an online viscosity detector. Due to the extremely low concentration, the intrinsic viscosity may be approximated by $(_{sp}/c$. The same analysis and experimental approach has recently been applied to *Sphagnum* pectins (Kristiansen, Ballance, Potthast, & Christensen, 2009), hyaluronan (Chytil, Strand, Christensen, & Pekar, 2010), chitosans (Christensen, Vold, & Vårum, 2008), and alginates (Vold et al., 2006). The pectin fractions show essentially linear MHS plots, in accordance with the MHS equation ($[\eta] = KM^a$), but with widely different slopes and vertical displacements.

CC1P2 and CC3 have different molar mass ranges, but their MHS plots fall roughly on the same line ($a = 0.6–0.7$), quite close to that of pullulan P1390. CC1P1 has a higher exponent in approximately the same area as alginate ($a = 0.8–0.9$). We attribute this high exponent to the effect of the pectin backbone (RG-I) which is quite stiff and resembles alginate (stiff) more than pullulan (flexible). Side chains will shift the exponent more toward a lower exponent, as clearly seen from the results of CC2 which diverse from the rest by having very low intrinsic viscosities, and also a low MHS exponent ($a = 0.3$), suggesting a compact structure, due to branching. This is in accordance with the linkage analysis where a much lower amount of branching points of Rha was detected (2.6%).

3.5. Sequencing of parts of the polymers by NMR

Due to the fact that CC1P1 has a fairly simple structure it was possible to unambiguously deduce the whole structure by NMR for this compound, see Table 3. The anomeric configuration of the monomers was partly based on coupling constants ($\alpha = 3.5$ Hz and $\beta = 8$ Hz) and comparison of the chemical shifts with data from the literature (Bock, Pedersen, & Pedersen, 1984; Bock & Thøgersen, 1983; Duus, Gotfredsen, & Bock, 2000). The $^3J^{CH}$ couplings seen in the HMBC spectra shows that the backbone in the molecule consists of α-GalA and α-Rha alternately linked as →4)αGalA (1→2) αRha(1→. This was also confirmed by weak hydrolysis of CC1P1 followed by the methylation analysis. Since the linkage between GalA and Rha is much more stable than the linkage to Gal, an appearance of 1→2Rha confirmed that the GalA is 1→2 linked to Rha. All terminal α-Gal is linked (1→3) to α-Rha, as shown by HMBC couplings in both directions. Normally Gal is present in β conformation, but here we report that T-Gal is present as α, being quite unusual in pectin structures. T-α-Gal has once before been found in pectins (Sengkhamparn, Bakx, et al., 2009) in the vegetable okra.

Neither $^3J^{CH}$ nor NOE couplings between were detected between GalA residues, indicating that homogalacturonan is not present. The results obtained from NMR are in accordance with the results from the methylation analysis and methanolysis. The structural information obtained from the different NMR experiments is illustrated in Fig. 4. The 3D model in Fig. 4a (ChemDraw 12, England) shows a small part of the molecule, $n = 12$. The polymer will not be present as stiff rods as the model indicates, but it will be flexible and present in solution as random coils as revealed by the SEC-MALLS and AFM results.

CC1P2 has a higher molecular weight, 1400 kDa, and is more complex and polydispers than CC1P1 (see Table 1). The high molecular weight also gives rise to a higher viscosity and this gives broadening of the NMR peaks. It is therefore difficult to assign all the chemical shifts of CC1P2. It was not possible to register a good HMBC spectrum, and for this reason the linkages between the monomers are based on analysis of the nuclear Overhauser effect (NOE) between different protons in the molecule and the chemical shifts. The assigned shifts can be found in Table 3(b). NOE couplings, showed some groups of monomers that are major building blocks in CC1P2 (Fig. 4b). By combining the results from linkage analysis, monosaccharide composition and NMR we found that all T-α-2-*O*Me-Gal (6.7%) are directly attached to α-Rha1→2,3 in position 3. This was showed by NOE cross peaks between α2-OMe-GalH1 (1→3) αRhaH3 and αRhaH1 (1→4) αGalAH4. This indicates that CC1P2 consists of approximately 20% 2)[α-2-OMe-Gal(1→3)]α-Rha(1→4)α-GalA(1→.

The strong NOE between H1 of 1→2,3Rha and H1 of T-α-4-OMe-GlcA indicates that these two are in close proximity to each other. This is possible if T-α-4-OMe-GlcA is linked through position 3 of 1→2,3 substituted Rha although we could not see NOE cross peaks between H3 of α-Rha1→2,3 and H1 of T-α-4-OMe-GlcA. It is also possible that parts of 4-OMe-GlcA can be linked to Rha1→2,4. Since CC1P2 only holds 15% Rha1→2,3, it is impossible that both 2-OMe-Gal and 4-OMe-GlcA only can be linked to this residue. Monosaccharide analysis shows 15% 4-OMe-GlcA, indicating that a large fraction of CC1P2 (approximately 50%) probably is composed of →2)[α-4-OMe-GlcA(1→3)]α-Rha(1→4)α-GalA(1→ or/and →2)[α-4-OMe-GlcA(1→4)]α-Rha(1→4)α-GalA(1→.

The same monosaccharide assembly as seen in CC1P1, →2)[α-Gal(1→3)]α-Rha(1→4)α-GalA(1→, was also detected for CC1P2

Table 3
(a) and (b) Chemical shifts assigned from dqCOSY, TOCSY, HSQC and ^{13}C NMR spectra of (a) CC1P1 and (b) CC1P2. Chemical shifts (δ, ppm) acetone 30.89/2.22 ppm.

	C1/H1	C2/H2	C3/H3	C4/H4	C5/H5	C6/H6	H6′	OMe
(a)								
→2.3) α L-Rhap (1→	98.60	76.80	77.00	72.17	69.30	16.80		
	5.25	4.19	4.01	3.70	3.84	1.26		
α T-D-Galp (1→	101.30	68.80	69.70	69.70	71.60	61.90		
	5.26	3.80	3.74	3.93	3.94	3.72	3.72	
→4) α-D-GalA (1→	97.80	68.20	70.60	77.80	72.00	176.00		
	5.01	3.88	4.12	4.44	4.48			
(b)								
→2.3) αRhapA (1→	99.00	77.10	78.10	72.40	70.20	17.20		
	5.31	4.16	3.97	3.60	3.80	1.25		
→2.3) αRhapB (1→	99.00	77.10	77.90	70.10				
	5.25	4.20	4.00	3.63	3.83	1.24		
T-αGalp (1→	101.70		70.10	70.10	71.40	62.20	62.20	
	5.26	3.79	3.72	3.90	4.06	3.71	3.71	
4→)αGalp (1→	101.70	70.00	69.10			61.70	61.70	
	5.24	3.78	3.85	3.93		3.71	3.84	
→4) α GalAp (1→	98.30	68.50	70.90	78.30	72.40			
	5.01	3.87	4.12	4.42	4.48			
T-α-2-OMe-Galp (1→	99.40	78.30	70.20	68.90		60.50		58.10
	5.40	3.51	3.92	3.92	3.74	3.85	3.85	3.49
T-α-4-OMe-GlcAp (1→	99.10	71.90	72.80	83.20	73.00			60.60
	4.98	3.57	3.78	3.20	4.14			3.48
→3.4) αGalAp (1→					72.10			
			4.10	4.45	4.83			

(see Fig. 4b). This might indicate that CC1P1 was not fully separated from CC1P2, or that this structure element also is a part of CC1P2. It is not possible to say in what extent this structural element is present as T-Gal also is a part of other side chains.

We did not succeed in assigning the chemical shift of C4 for 1→4 linked α-Gal present, see Table 3(b). Assigning this chemical shift would make it possible to deduce which residue 1→4 linked α-Gal is linked to. Unfortunately, H4 of α-Gal (1→4) comes in the most crowded region of the NMR spectra, with a lot of overlaying signals making it difficult to make assumptions solely on this signal. The chemical shift of H1 (δ 5.24) indicates that all 1→4 linked Gal unites are present in α configuration, which to the knowledge of the authors not has been detected before in pectins. Since NMR is not a very sensitive method, it is difficult to detect monosaccharides that are present in many different electronic environments, i.e. galactans or AG-I.

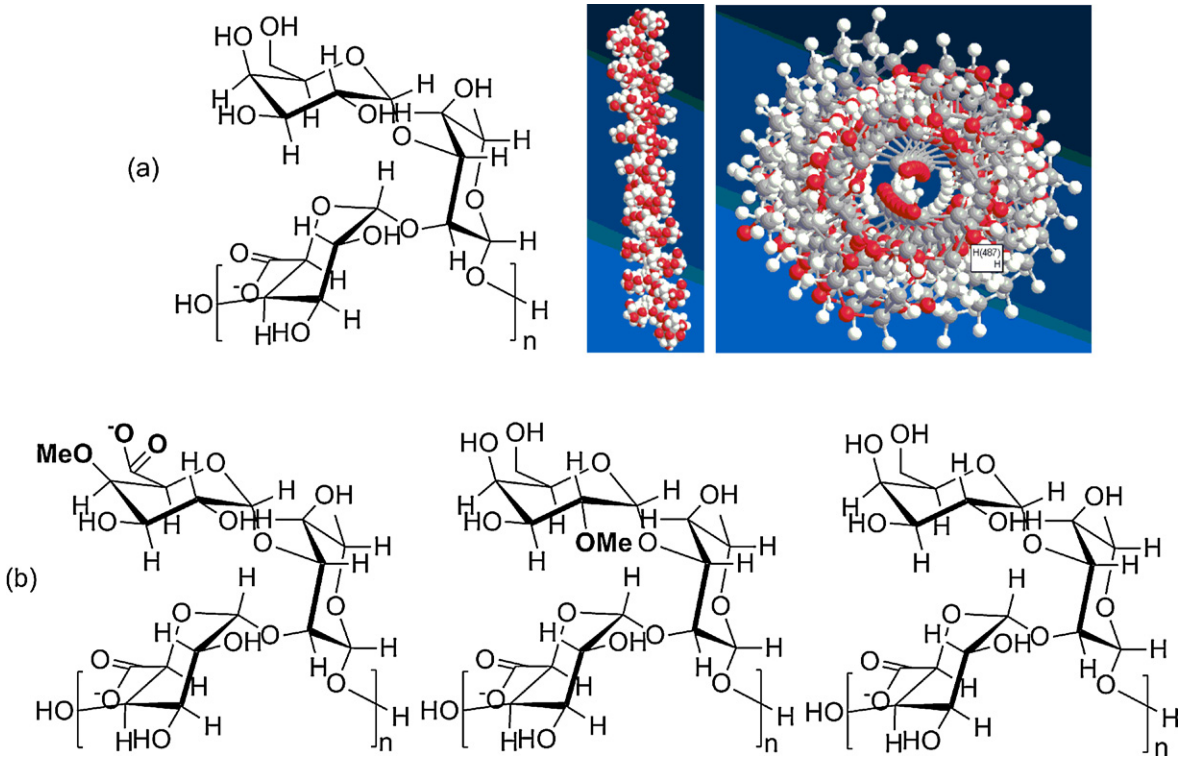

Fig. 4. (a) The structure of CC1P1 as showed in chair formation and 3D. HMBC $^{3}J^{CH}$ couplings were observed between the following residues: αGalA C1 (1→2) αRha H2, αGalA C4 (4→1) αRha H1, αGal C1 (1→3) αRha H3, αRha C3 (3→1) αGal H1. Molecular modeling (MM2), has been applied for 3D images. (b) Structural elements of CC1P2 as shown by NMR and GC/MS.

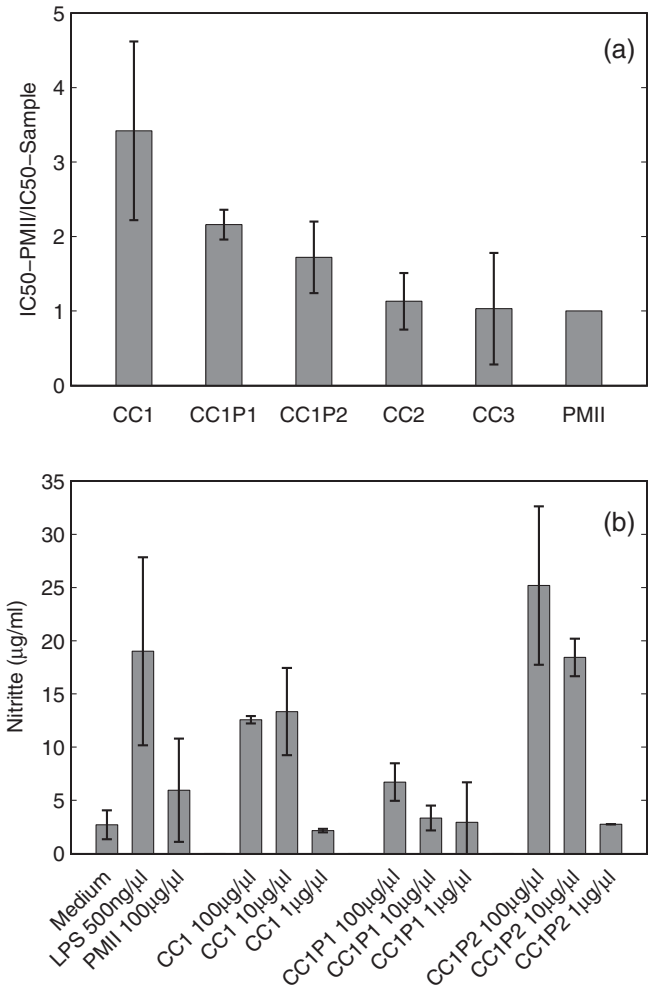

Fig. 5. (a) and (b) Biological activity. (a) Complement fixation assay. The figure shows the ratio IC_{50}-PMII/IC_{50}-sample and thus shows how active each individual test sample is compared to the positive control, PMII. These results are based on three separate experiments. CC1 and CC1P1 is significantly more active that PMII ($p < 0.05$). (b) Stimulation of macrophages. A representative result is given as mean ± SD. LPS and PMII are present as positive controls.

3.6. Structure–activity relationship

The fractions were tested in two immunological in vitro test systems. The two systems focus on different parts of the immune system, the complement system and the macrophages, which both are parts of the innate immune system. 1→3,6-β-galactans (AG-II) structures are often present in immunomodulating polysaccharide of plant origin (Paulsen & Barsett, 2005; Yamada & Kiyohara, 2007). Ramified regions (hairy regions) of RG-I and RG-II type are also important for activity.

All *C. cordifolia* polysaccharide fractions exhibit the same or higher complement-fixing activity, see Fig. 5, compared to the very positive control PMII (Samuelsen et al., 1996), in a dose-depended manner (data not shown). PMII is a RG-I type pectin with AG-II side chains, and is also containing homogalacturonan sections. We use this plant polysaccharide isolated from *P. major* as a positive control in bioassays representing typical plant pectin with bioactivity in the relevant assays.

CC1 exhibits a higher complement-fixing activity than any of its sub-fractions, which can be explained by a possible synergistic effect between the polysaccharide present in CC1, which then will enhance the response in the assay. Another reason for the relative high activity of CC1 might be that it contains tannins that will interfere with the assay and give false increased positive response (Wagner et al., 1999). In this case, as the highly purified CC1P1 and CC1P2 also have a high activity, a majority of the activity present in CC1 must arise from the polysaccharides present.

Although CC1P1 has a lower activity compared to CC1, the activity is still considered high (2.2 times more active than the positive control, PMII, $p < 0.05$). CC1P1 has not any of the structural elements regarded as important for structure activity in the literature (Yamada & Kiyohara, 2007), as the backbone consists of 1→2,3 linked Rha, not 1→2,4 linked as normally present in pectins. Additionally, all Gal is α-linked and present as single units, a structural element that not has been tested in these bioassays before. Normally, side chains consist of several monosaccharides. Complement modulating activity has never before been reported for pectin-like polymers with such an uncommon and well defined structure as CC1P1 has. CC1P2, which is more complex with both 4-OMe-GlcA and 2-OMe-Gal in terminal positions, is approximately 2 times more active than PMII. This polysaccharide has also branching on GalA, which also might be of importance; this has previously been shown for polysaccharides present in the Malian medicinal plant *Combretum glutinosum* (Glæserud et al., 2011). CC3 has some of the same structural elements as present in CC1P2, but a much lower M_w (65 kDa). The activity of CC3 has probably a lower activity than CC1P2, which might indicate that the molecular weight is important for activity.

The activity of CC2 is in the same magnitude as the positive control, PMII. Structurally, CC2 resembles normal pectins, with typical AG-II structures, but it also include 6.6% 4-O-Me-GlcA and some 1→2,3 linked Rha. Since CC2 has a high degree of AG-II regions and a small amount of homogalacturonan we expected an even higher activity in the complement system (Yamada & Kiyohara, 1999). Homogalacturonan is often considered inactive, but has also been referred to as a structural element that might be of importance for keeping the molecule in the correct configuration for optimal activity (Inngjerdingen et al., 2007; Nergaard et al., 2005).

The ability of the polymers to stimulate the mouse macrophages to produce NO is shown in Fig. 5(b). NO is a good marker for macrophage activation, and its stable breakdown product nitrite can easily be detected in culture supernatants. As opposed to the results from the complement test, CC1P2 is highly active while CC1, being a mixture of CC1P1 and CC1P2, has a lower activity. Preliminary experiments carried out on CC3 showed no activity (results not shown), which might indicate that a high Mw is of importance since CC1P2 (1400 kDa) and CC3 (65 kDa) has a similar linkage and monosaccharide composition (see Table 2). One reason for the high effect of CC1P2 might be contributed to the 7% branching points on GalA. Glæserud et al. (2011) showed that substitutions on GalA in the backbone increased the activity. The branching on GalA for CC1P2 is not a part of RG-II.

CC1P1 shows no significant effect in this system which might indicate that activation of macrophages is dependent on longer side chains than those present in CC1P1. The almost non existing macrophage activation by CC1P1 also strongly suggests that LPS is not present in interfering amounts in our fractions, as all fractions are derived from the same extract.

None of the fractions showed any signs of cytotoxicity toward human fibroblasts after 24 h of exposure as shown by LDH test. *C. cordifolia* is often applied locally on wounds and it is therefore important that the extract is non-cytotoxic toward human fibroblasts (skin cells).

4. Conclusion

The main goal of this study was to investigate the structure–activity relationship of the pectic like polymers present in the bark of *C. cordifolia* by the use of GC, GC/MS, SEC-MALLS, NMR

and in vitro immunological assays. In a previous study (Togola et al., 2008) advanced structural elucidation and purification was not possible because of interfering cations. Removing divalent ions by the use of a strong solid-phase chelator gave polysaccharides that did not aggregate, and fractionation and chemical elucidation of the fine structure was possible. The sub fractions had quite different chemical structures and molecular weights, and a new type of pectic structure was identified consisting of the repeating structure [2→)[α-D-Gal(1→3)]α-L-Rha(1→4)α-D-GalA(1→]. The presence of α-linked Gal is unusual. The other structures were also different from pectic structures normally found in the plant kingdom. The different fractions have all a substantial effect in the complement assay, and the most unusual ones did also have the ability to stimulate NO production in macrophages. The results indicate that the structural elements important for complement activation are not always important for macrophage activation. The chain length and types of linkages and availability of active sites also influence the activity.

Acknowledgments

The first author acknowledges Dr. Fuad Fares, Israel, for the opportunity of working in his lab to carry out the cytotoxicity test, Per Eugen Kristiansen and Frode Rise, University of Oslo, Norway, for help with recording NMR spectra and Finn Tønnesen for recording the GC/MS data, Suthajini Yogarajah for carrying out the methylation analysis of CC2, and EMBIO for financing the visit to Dr. Fuad Fares lab and Ann-Sissel Ulset and Fen Qin, NTNU, Trondheim, Norway, for help performing the SEC-MALLS experiments. The NMR experiments were carried out at the Danish Instrument Center for NMR Spectroscopy of Biological Macromolecules.

References

Bock, K., Pedersen, C., & Pedersen, H. (1984). C-13 nuclear magnetic-resonance data for oligosaccharides. *Advances in Carbohydrate Chemistry and Biochemistry*, *42*, 193–225.

Bock, K., & Thøgersen, H. (1983). Nuclear magnetic resonance spectroscopy in the study of mono- and oligosaccharides. *Annual Reports on NMR Spectroscopy*, *13*, 1–57.

Chambers, R. E., & Clamp, J. R. (1971). Assessment of methanolysis and other factors used in the analysis of carbohydrate-containing materials. *Biochemical Journal*, *125*(4), 1009–1018.

Christensen, B. E., Ulset, A. S., Beer, M. U., Knuckles, B. E., Williams, D. L., Fishman, M. L., et al. (2001). Macromolecular characterisation of three barley [beta]-glucan standards by size-exclusion chromatography combined with light scattering and viscometry: An inter-laboratory study. *Carbohydrate Polymers*, *45*, 11–22.

Christensen, B. E., Vold, I. M. N., & Vårum, K. M. (2008). Chain stiffness and extension of chitosans and periodate oxidised chitosans studied by size-exclusion chromatography combined with light scattering and viscosity detectors. *Carbohydrate Polymers*, *74*, 559–565.

Chytil, M., Strand, S., Christensen, B. E., & Pekar, M. (2010). Calorimetric and light scattering study of interactions and macromolecular properties of native and hydrophobically mod. *Carbohydrate Polymers*, *81*(4), 855–863.

Ciucanu, I., & Kerek, F. (1984). A simple and rapid method for the permethylation of carbohydrates. *Carbohydrate Research*, *131*(2), 209–217.

Classen, B., Thude, S., Blaschek, W., Wack, M., & Bodinet, C. (2006). Immunomodulatory effects of arabinogalactan-proteins from *Baptisia* and *Echinacea*. *Phytomedicine*, *13*(9–10), 688–694.

Diallo, D., Sogn, C., Samake, F. B., Paulsen, B. S., Michaelsen, T. E., & Keita, A. (2002). Wound healing plants in Mali, the Bamako region. An ethnobotanical survey and complement fixation of water extracts from selected plants. *Pharmaceutical Biology*, *40*(2), 117–128.

Dubois, M., Gilles, K. A., Hamilton, J. K., Rebers, P. A., & Smith, F. (1956). Colorimetric method for determination of sugars and related substances. *Analytical Chemistry*, *28*, 350–356.

Duus, J., Gotfredsen, C. H., & Bock, K. (2000). Carbohydrate structural determination by NMR spectroscopy: Modern methods and limitations. *Chemical Review*, *100*(12), 4589–4614.

Glæserud, S., Gronhaug, T. E., Michaelsen, T. E., Inngjerdingen, M., Barsett, H., Diallo, D., et al. (2011). Immunomodulating polysaccharides from leaves of the Malian medicinal tree *Combretum glutinosum*; structural differences between small and large leaves can substantiate the preference for small leaves by some healers. *Journal of Medicinal Plants Research*, *5*(13), 2781–2790.

Goddard, T. D., & Kneller, D. G. (2009). *Sparky 3*. University of California: San Francisco.

Grønhaug, T. E., Glaeserud, S., Skogsrud, M., Ballo, N., Bah, S., Diallo, D., et al. (2008). Ethnopharmacological survey of six medicinal plants from Mali, West-Africa. *Journal of Ethnobiology and Ethnomedicine*, *4*, 26.

Inngjerdingen, K. T., Patel, T. R., Chen, X., Kenne, L., Allen, S., Morris, G. A., et al. (2007). Immunological and structural properties of a pectic polymer from *Glinus oppositifolius*. *Glycobiology*, *17*(12), 1299–1310.

Kim, J. B., & Carpita, N. C. (1992). Changes in esterification of the uronic-acid groups of cell-wall polysaccharides during elongation of maize coleoptiles. *Plant Physiology*, *98*(2), 646–653.

Kim, L. S., Waters, R. F., & Burkholder, P. M. (2002). Immunological activity of larch arabinogalactan and *Echinacea*: A preliminary, randomized, double-blind, placebo-controlled trial. *Alternative Medicine Review*, *7*(2), 138–149.

Kristiansen, K. A., Ballance, S., Potthast, A., & Christensen, B. E. (2009). An evaluation of tritium and fluorescence labelling combined with multi-detector SEC for the detection of carbonyl groups in polysaccharides. *Carbohydrate Polymers*, *76*(2), 196–205.

Limansky, A. P., Shlyakhtenko, L. S., Schaus, S., Henderson, E., & Lyubchenko, Y. L. (2002). Aminomodified probes for atomic force microscopy. *Probe Microscopy*, *2*(3), 227–234.

Michaelsen, T. E., Gilje, A., Samuelsen, A. B., Hagasen, K., & Paulsen, B. S. (2000). Interaction between human complement and a pectin type polysaccharide fraction, PMII, from the leaves of *Plantago major* L. *Scandinavian Journal of Immunology*, *52*(5), 483–490.

Morris, V. J., Gromer, A., Kirby, A. R., Bongaerts, R. J. M., & Gunning, A. P. (2011). Using AFM and force spectroscopy to determine pectin structure and (bio) functionality. *Food Hydrocolloids*, *25*(2), 230–237.

Naran, R., Chen, G., & Carpita, N. C. (2008). Novel rhamnogalacturonan I and arabinoxylan polysaccharides of flax seed mucilage. *Plant Physiology*, *148*, 132–141.

Nergaard, C. S., Kiyohara, H., Reynolds, J. C., Thomas-Oates, J. E., Matsumoto, T., Yamada, H., et al. (2005). Structure-immunomodulating activity relationships of a pectic arabinogalactan from *Vernonia kotschyana* Sch. Bip. ex Walp. *Carbohydrate Research*, *340*(11), 1789–1801.

Paulsen, B. S., & Barsett, H. (2005). Bioactive pectic polysaccharides. *Advances in Polymer Science*, *186*, 69–101.

Perez, S., Rodriguez-Carvajal, M. A., & Doco, T. (2003). A complex plant cell wall polysaccharide: Rhamnogalacturonan II. A structure in quest of a function. *Biochimie*, *85*(1–2), 109–121.

Popov, S. V., Popova, G. Y., Ovodova, R. G., Bushneva, O. A., & Ovodov, Y. S. (1999). Effects of polysaccharides from Silene vulgaris on phagocytes. *International Journal of Immunopharmacology*, *21*(9), 617–624.

Samuelsen, A. B., Paulsen, B. S., Wold, J. K., Otsuka, H., Kiyohara, H., Yamada, H., et al. (1996). Characterization of a biologically active pectin from *Plantago major* L. *Carbohydrate Polymers*, *30*, 37–44.

Sengkhamparn, N., Bakx, E. J., Verhoef, R., Schols, H. A., Sajjaanantakul, T., & Voragen, A. G. J. (2009). Okra pectin contains an unusual substitution of its rhamnosyl residues with acetyl and alpha-linked galactosyl groups. *Carbohydrate Research*, *344*(14), 1842–1851.

Sengkhamparn, N., Verhoef, R., Schols, H. A., Sajjaanantakul, T., & Voragen, A. G. J. (2009). Characterisation of cell wall polysaccharides from okra (*Abelmoschus esculentus* (L.) Moench). *Carbohydrate Research*, *344*(14), 1824–1832.

Sweet, D. P., Shapiro, R. H., & Albersheim, P. (1975). Quantitative-analysis by various glc response-factor theories for partially methylated and partially ethylated alditol acetates. *Carbohydrate Research*, *40*(2), 217–225.

Togola, A., Paulsen, B. S., Naess, K. H., Diallo, D., Barsett, H., & Michaelsen, T. E. (2008). A polysaccharide with 40% mono-O-methylated monosaccharides from the bark of *Cola cordifolia* (Sterculiaceae), a medicinal tree from Mali (West Africa). *Carbohydrate Polymers*, *73*(2), 280–288.

Tomoda, M., Nakatsuk, S., & Satoh, N. (1974). Plant mucilages: Location of o-acetyl groups and nature of branches in bletilla-glucomannan. *Chemical & Pharmaceutical Bulletin*, *22*(11), 2710–2713.

van Holst, G. J., & Clarke, A. E. (1985). Quantification of arabinogalactan-protein in plant extracts by single radial gel diffusion. *Analytical Biochemistry*, *148*(2), 446–450.

Vold, I. M. N., Kristiansen, K. A., & Christensen, B. E. (2006). A study of the chain stiffness and extension of alginates, in vitro epimerized alginates, and periodate-oxidized alginates using size-exclusion chromatography combined with light scattering and viscosity detectors. *Biomacromolecules*, *7*(7), 2136–2146.

Wagner, H., Kraus, S., & Jurcic, K. (1999). *Search for potent immunostimulating agents from plants and other natural sources*. Berlin: Birkhaüser Verlag.

Welz, B., & Sperling, M. (1999). *Atomic absorption spectrometry*. Weinheim: Wiley-VCH.

Yamada, H., & Kiyohara, H. (1999). Complement-activating polysaccharides from medicinal herbs. In H. Wagner (Ed.), *Immunomodulatory Agents from Plants* (pp. 161–202). Basel: Birkhauser.

Yamada, H., & Kiyohara, H. (2007). Immunomodulating activity of plant polysaccharide structure. In J. P. Kamerling (Ed.), *Comprehensive glycoscience* (pp. 663–693). Oxford, UK: Elsevier Ltd.

Yamada, H., Kiyohara, H., & Marsumoto, T. (2009). Recent studies on structures and intestinal immunity modulating actiities of pectins and pectic polysaccharides. In H. Schols, R. G. F. Visser, & A. G. J. Voragen (Eds.), *Pectins and pectinases* (pp. 293–304). Wageningen: Wageningen Academic Publishers.